JCB Article

Local ERM activation and dynamic growth cones at Schwann cell tips implicated in efficient formation of nodes of Ranvier

Cheryl L. Gatto, Barbara J. Walker, and Stephen Lambert

Department of Cell Biology and Program in Neuroscience, University of Massachusetts Medical School, Worcester, MA 01605

Nodes of Ranvier are specialized, highly polarized axonal domains crucial to the propagation of saltatory action potentials. In the peripheral nervous system, axo–glial cell contacts have been implicated in Schwann cell (SC) differentiation and formation of the nodes of Ranvier. SC microvilli establish axonal contact at mature nodes, and their components have been observed to localize early to sites of developing nodes. However, a role for these contacts in node formation remains controversial.

Using a myelinating explant culture system, we have observed that SCs reorganize and polarize microvillar components, such as the ezrin-binding phosphoprotein 50 kD/regulatory cofactor of the sodium-hydrogen exchanger isoform 3 (NHERF-1), actin, and the activated ezrin, radixin, and moesin family proteins before myelination in response to inductive signals. These components are targeted to the SC distal tips where live cell imaging reveals novel, dynamic growth cone–like behavior. Furthermore, localized activation of the Rho signaling pathway at SC tips gives rise to these microvillar component–enriched "caps" and influences the efficiency of node formation.

Introduction

Myelination is a vertebrate adaptation, which involves a specialized glial cell generating an insulating, multilamellar sheath around an associated axon (for reviews see Arroyo and Scherer, 2000; Scherer and Arroyo, 2002). This is coupled with the specific localization of voltage-gated sodium channels (vgsc's) to gaps in the myelin sheath known as the nodes of Ranvier. As these channels are enriched in this domain at concentrations of minimally 40-fold excess as compared with internodal regions, the electrical requirements to promote rapid, saltatory conduction of action potentials are met while sparing a concomitant increase in axonal caliber (Ritchie and Rogart, 1977; Shrager, 1989).

The development of the nodes of Ranvier not only involves substantial morphological alterations in the myelinating glial cell but is also hallmarked by the discrete polarization of axonal cell adhesion molecules, cytoskeletal components, and ion channels. Upon myelination, the L1 cell adhesion molecule, the 155-kD isoform of neurofascin, and the cytoskeletal protein ankyrin$_B$ are down-regulated and removed from the axonal plasma membrane. Conversely, the 186-kD isoform of neurofascin and Nr-CAM become highly localized to the node in association with ankyrin$_G$ and vgsc's (Martini and Schachner, 1986; Kordeli et al., 1995; Davis et al., 1996; Lambert et al., 1997).

The role of axo–glial contacts in promoting vgsc clustering at the node remains controversial. vgsc clusters have been observed in the axons of retinal ganglion cells cultured in the presence of oligodendrocyte conditioned media but in the absence of cellular contact (Kaplan et al., 1997). Similarly, observations of vgsc clusters in amyelinated regions of axons from the *dystrophic* mouse (Deerinck et al., 1997) support the hypothesis that vgsc clustering is independent of glial cell contacts. However, in vitro myelinating culture studies have shown a requirement for Schwann cell (SC) contacts in mediating axonal vgsc clustering (Ching et al., 1999). This is supported by in vivo observations showing that vgsc and other nodal proteins cluster in close proximity to myelin-

The online version of this article includes supplemental material.

Address correspondence to Stephen Lambert, Dept. of Cell Biology, University of Massachusetts Medical School, 4 Biotech, 377 Plantation St., Suite 326, Worcester, MA 01605. Tel.: (508) 856-8665. Fax: (508) 856-8774. email: Stephen.Lambert@umassmed.edu

Key words: glial cells; nodes of Ranvier; myelin sheath; growth cones; microvilli

Abbreviations used in this paper: BME, basal medium Eagle's; DRG, dorsal root ganglion; EBP50, ezrin-binding phosphoprotein 50 kD; ERM, ezrin, radixin, and moesin family proteins; LPA, lysophosphatidic acid; MAG, myelin-associated glycoprotein; MBP, myelin basic protein; ROCK, Rho-associated kinase; SC, Schwann cell; vgsc, voltage-gated sodium channel.

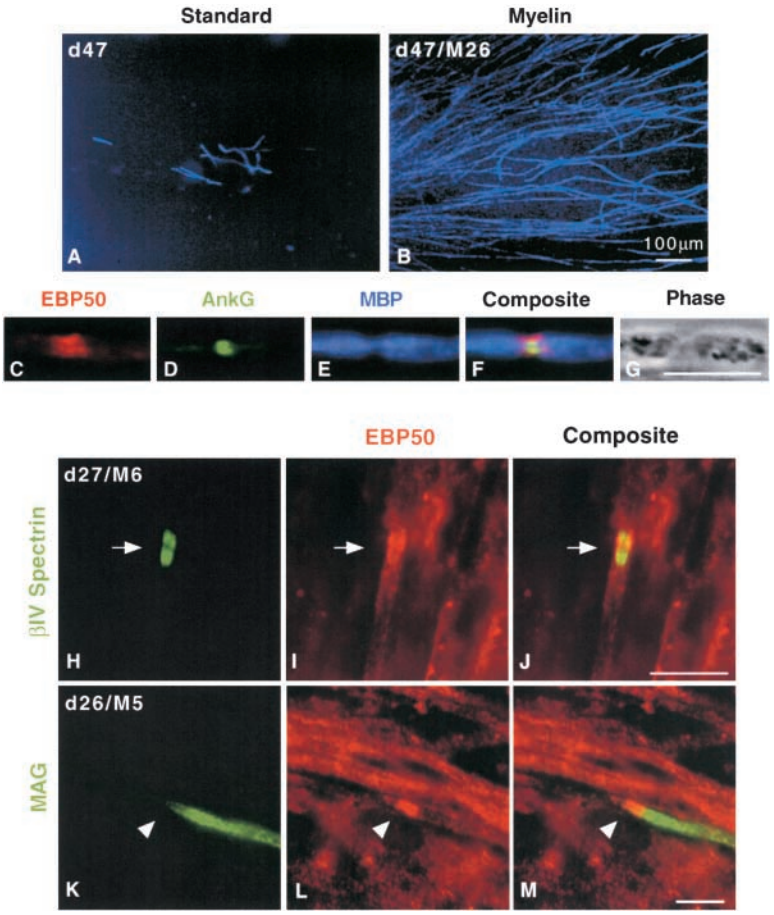

Figure 1. **EBP50/ERM localization to early and mature nodes in myelinating DRG explant cultures.** (A, ST:d47; B, MY:d47/M26) Myelinated and comparable control cultures were stained for MBP to show mature myelin. (C–E) EBP50/Ank_G/MBP revealed nodal specializations. (F) Note that SC microvillar EBP50 staining encompassed axonal Ank_G. Less differentiated cultures (M5/6) were stained with EBP50 (I and L) and either βIV spectrin (H, axonal marker) or MAG (K, early myelin marker). (M and J) EBP50 was clearly present at early hemi- (arrowheads) and binary (arrows) nodes. Bars, 10 μm except where indicated.

associated glycoprotein (MAG)-positive SC processes (Vabnick et al., 1996; Lambert et al., 1997) during myelination of the sciatic nerve. Mechanisms underlying these apparently conflicting lines of evidence remain to be determined.

In the mature peripheral nervous system, axo–glial contacts at the nodes of Ranvier are established by SC microvilli (Ichimura and Ellisman, 1991), characterized by expression of F-actin (Trapp et al., 1989), ezrin, radixin, and moesin family proteins (ERMs), and ezrin-binding phosphoprotein 50 kD (EBP50; Melendez-Vasquez et al., 2001; Scherer et al., 2001). To investigate a potential role for these microvilli in node formation, we have studied their formation in myelinating dorsal root ganglion (DRG) explant cultures. We have observed that myelinating SCs polarize microvillar components to novel structures at their distal tips (termed caps) in response to signals that induce myelin formation. These caps are enriched in microvillar components including EBP50, actin, and activated phospho-ERMs. Using EBP50-GFP as a probe in live cell imaging experiments, we observed that SC caps are highly dynamic with behavior reminiscent of an axonal growth cone. We also localized the small GTPase RhoA to the SC cap and found that activation of the Rho pathway was linked to cap formation. Together, these results suggest a localized Rho-mediated activation of ERM proteins at the SC cap. Furthermore, the uncoupling of cap formation and myelination interfered with efficient node formation implicating the SC as having a direct role in establishment of the nodes of Ranvier.

Results

Localization of microvillar components at SC tips is an early event in the myelin program

Here, myelinating DRG explants were used to examine SC differentiation and formation of the nodes of Ranvier. This system allowed for the controlled induction of myelination upon the addition of serum and ascorbate to the culture media. This enabled the consistent generation of substantially myelinated cultures, as indicated by myelin basic protein (MBP) staining to reveal compacted myelin (Fig. 1 B). Occasionally, small numbers of segments were also observed in cultures maintained in standard feed (Fig. 1 A). When present, these segments were aberrantly short with irregular morphology and inconsistent nodal association.

To follow the evolution of nodal SC microvilli in our myelinating cultures, we generated an antibody to EBP50. EBP50 was observed to localize to the SC nodal collar of microvilli in mature myelinated cultures (47 total days in culture/26 d after induction of myelination with serum and ascorbate [d47/M26]), confirming in vivo observations in mature sciatic nerve (Melendez-Vasquez et al., 2001). Staining at the nodal regions illustrated EBP50 encompassing $ankyrin_G$, which is known to localize to the electron dense undercoating at the nodal axolemma (Kordeli et al., 1990; Fig. 1, C–G).

EBP50 polarization in less differentiated cultures was then examined. MAG, which is expressed abaxonally by myelin-

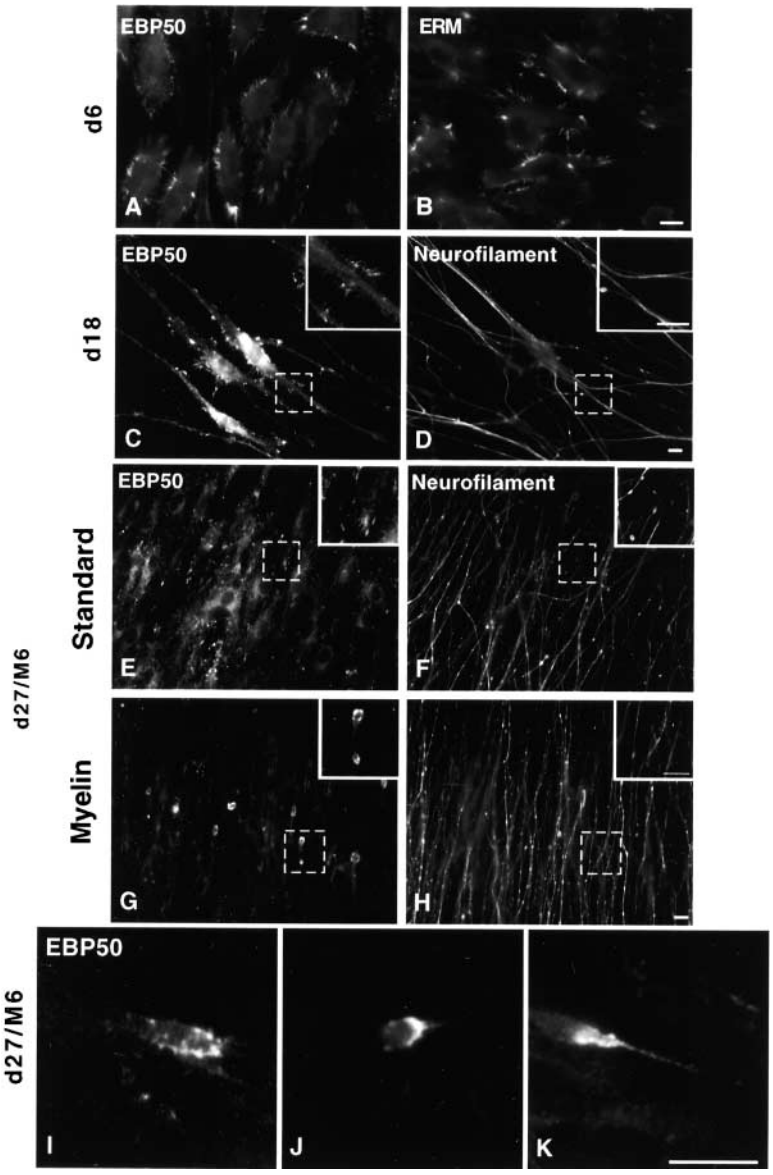

Figure 2. **EBP50/ERM localization in premyelinating/induced DRG explant cultures changes from cell surface microvilli to a focal concentration at the SC tip.** After 6 d in vitro, cultures were stained for (A) EBP50 and (B) ERM. Note the numerous cell surface microvilli present on migrating SC. After 18 d, cultures were stained for (C) EBP50 and (D) neurofilament. Bipolar SCs displayed microvilli along their length. Matched standard cultures (d27) and cultures induced to myelinate with serum and ascorbate (d27/M6) were stained for (E and G) EBP50 and (F and H) neurofilament. There was discrete localization of EBP50 to SC tips in the induced cultures. (I–K) These EBP50-positive tips were also found with varying morphologies. Bars, 10 μm.

ating SCs after ~1.5 wraps around its associated axon (Martini and Schachner, 1986, 1988), was used to visualize earlier stages of myelination. After 5–6 d of induction, EBP50 localized to both heminodal and binary intermediates adjacent to MAG-positive SCs (Fig. 1 M) and in close proximity to axonal clusters of βIV spectrin (Fig. 1 J), a second marker for the axonal nodal membrane (Berghs et al., 2000; Komada and Soriano, 2002). These results indicate a distinct localization of microvillar components, if not microvilli proper, at mature and developing nodes.

The three ERM proteins (ezrin, radixin, and moesin) are present in SC microvilli (Melendez-Vasquez et al., 2001; Scherer et al., 2001). Hence, we used a pan-ERM antibody in conjunction with our EBP50 antibody to examine microvillar organization in developing SCs. After 6 d in vitro, EBP50 and ERM staining revealed numerous microvilli (Fig. 2, A and B) covering the surface of migrating SC precursors. Mature SCs, characterized by a bipolar phenotype (Jessen et al., 1994), also exhibited numerous microvilli decorating their length (Fig. 2 C).

Cultures were supplemented with 15% serum and 50 μg/ml ascorbate to promote myelination (Eldridge et al., 1987), and a dramatic reorganization of the SC microvilli was seen. Upon induction (d27/M6), EBP50 staining became concentrated at the distal tips of the elongated SCs (Fig. 2 G), which was not observed in equivalent control cultures (Fig. 2 E). Notable variations in tip morphology and EBP50 localization were also observed, suggesting a dynamic component involved in cap formation (Fig. 2, I–K).

Live cell imaging reveals the existence of a novel, dynamic "growth cone"–like structure at the tips of myelinating SCs

To visualize the dynamics of cap formation in live cells, an EBP50-GFP fusion construct was used. When transfected into myelinating DRG cultures, this construct was observed to localize to cap structures at SC tips (Fig. 3 A). Moreover, this localization required the ERM binding site of EBP50 (unpublished data). As the binding site for EBP50 is masked

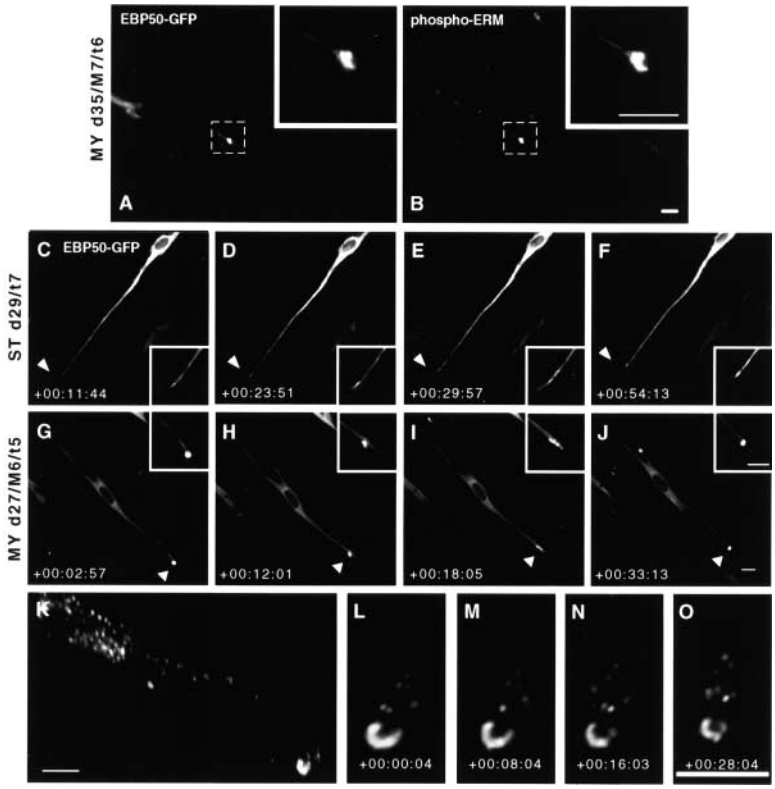

Figure 3. **Dynamic EBP50/ERM-positive SC distal tips.** Cultures were transfected after 1 d of induction. After 5 d of transfection, (A) EBP50-GFP was seen to colocalize with (B) endogenous phospho-ERM staining at SC tips. These transfected cultures were then examined via time-lapse microscopy. (C–F) SCs in standard cultures (d29/t7) showed no specific localization of EBP50-GFP at their tips (arrows). (G–J) SC in myelinating cultures (d29/M6/t5) had dynamic, remodeling EBP50-GFP–positive tips (arrowheads). (K–O) Furthermore, deconvolution microscopy revealed EBP50-GFP as having a punctate distribution. Bars, 10 μm.

on inactive ERM molecules (Gary and Bretscher, 1995; Matsui et al., 1998), these results suggest that localization of EBP50-GFP to SC caps reflects the local activation of ERM molecules at these sites. In support of this idea, EBP50-GFP was found to colocalize with COOH-terminal phospho-ERM staining (Fig. 3 B), indicative of active forms of these proteins (Reczek et al., 1997; Reczek and Bretscher, 1998).

Time-lapse imaging of explants harboring EBP50-GFP transfected SCs demonstrated the dynamics of the EBP50-positive tips. Cultures sustained in standard feed (d29/t7) maintained EBP50-GFP diffusely throughout the cytoplasm without any distinctive localization (Fig. 3, C–F; Videos 1 and 2 are available at http://www/jcb.org/cgi/content/full/jcb.200303039/DC1). Notably, these EBP50-GFP–transfected SC appear smoother than comparable EBP50-stained SC under standard conditions (Fig. 2 C). Due to the lower magnifications used for time-lapse imaging and overexpression of the construct, fluorescence from the cell body overwhelms the signal contributed from the fine microvilli along the SC length. However, in cultures supplemented to promote myelination (d27/M6/t5), EBP50-GFP became highly localized to SC tips and displayed active remodeling (Fig. 3, G–J; Videos 3 and 4 are available at http://www/jcb.org/cgi/content/full/jcb.200303039/DC1). Deconvolution microscopy demonstrated EBP50-GFP in a punctate distribution throughout the cell body, as well as concentrating at SC tips (Fig. 3, K–O).

To determine whether the GFP-remodeling reflected actual changes in the morphology of the SC tip, we studied acutely dispersed SC preparations. This allowed for visualization of individual cells that was not possible without transfection in explants due to the culture complexity. As observed in explant SCs, isolated bipolar cells displayed discrete tips enriched in microvillar components, such as EBP50 and actin (Fig. 4, A–H). Furthermore, the tip-localizing ERMs were again found to be enriched in the activated versions of these proteins (Fig. 4, I–L), whereas nonphosphorylated ERMs were diffusely present in the SC body and processes (Fig. 4, M–P). Concentrations of RhoA were also observed at the SC tips (Fig. 4, Q–T). Specifically, 79.1 ± 1.7% (data presented as mean ± SEM) of SC tips that were positively immunostained for either EBP50 or phospho-ERM also displayed accumulations of RhoA.

As explant studies demonstrated the specific rearrangement of EBP50 at SC tips, isolated SCs were imaged to examine the general nature of the cells' distal region. SC tips were reminiscent of actively remodeling axonal growth cones. Isolated cells revealed significant detail including the elaboration of lamellipodia and extension of filopodia (Fig. 5). We hypothesize that these SC distal tips may serve as novel glial growth cone–type structures that enable axonal recognition and segregation, as well as the establishment of early nodes in the process of myelination.

Local activation of Rho signaling pathway at SC tips gives rise to caps and influences node formation

SC caps were observed to form in response to culture conditions that promoted myelination in DRG explant cultures, namely the addition of serum and ascorbate. To determine which of these components stimulated cap formation, cultures were independently supplemented with either serum or ascorbate. It was observed that the presence of serum was required for cap formation in studies of endogenous EBP50 staining (Fig. 6, A–D). Quantitative

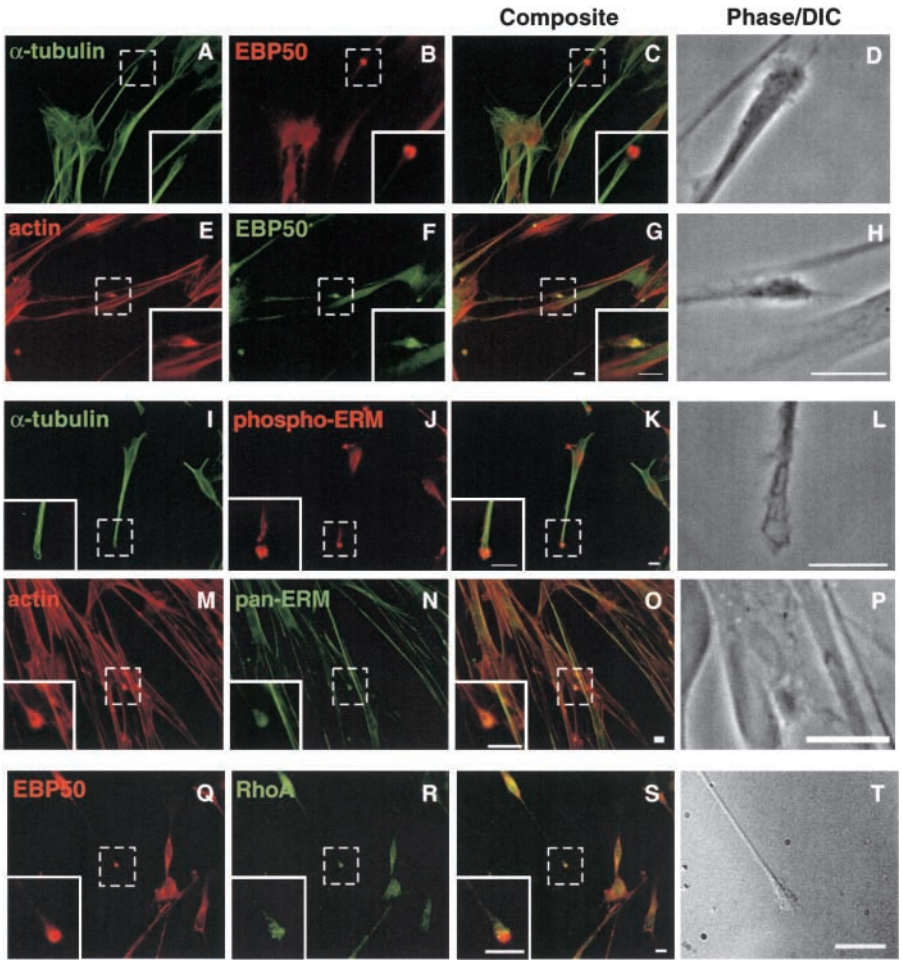

Figure 4. **EBP50, actin, activated ERMs, and RhoA localize to SC tips.** Isolated SCs were stained to identify other proteins residing at the tips. (A–C) EBP50 was found at the tip of α-tubulin containing SC processes. (E–G) Actin colocalized with EBP50 at the SC tip, as did activated, phospho-ERMs (I–K). Pan-ERM antibody staining revealed ERMs generally present at the SC tips. However, this staining was less concentrated at these sites than is observed with activated ERMs and more diffusely localized throughout the SC body and processes (M–O). (Q–S) In addition, the small GTPase RhoA localized generally to the SC distal tip in close proximity to EBP50. The tips examined also have corresponding magnified views of either (D, H, L, and P) phase or (T) DIC shown to detail tip morphologies. Quantitatively, 79.1 ± 1.7% (mean ± SEM) of EBP50 or phospho-ERM reactive SC tips displayed distal RhoA accumulations. Bars, 10 μm.

analysis of this phenomenon using EBP50-GFP transfection experiments (Fig. 6, E–L) revealed that the presence of serum induced a five- to sixfold increase in the number of EBP50-positive caps as compared with ascorbate alone. Furthermore, ascorbate alone was as ineffective as standard feed in inducing cap formation (2.8 ± 0.8% vs. 2.3 ± 0.6%, respectively), whereas serum alone produced similar results as compared with complete myelin feed (serum + ascorbate) in promoting cap formation (11.6 ± 0.7% vs. 14.2 ± 1.1%, respectively; Fig. 6).

ERM activation has been demonstrated to be downstream of Rho activity (Matsui et al., 1998; Shaw et al., 1998; Yonemura et al., 2002). Our observations, including the effects of serum and Rho localization, implicate a local activation of the Rho pathway in cap formation. Therefore, we used the serum phospholipid lysophosphatidic acid (LPA) to determine whether or not RhoA pathway activation affected cap formation. LPA has been shown to stimulate Rho-dependent pathways influencing cytoskeletal architecture in various cell types, including SCs (Weiner et al., 2001). Cultures were treated with 1 μM LPA or 1 μM LPA + 50 μg/ml ascorbate. It was observed that LPA was able to compensate for an omission of whole serum from the culture medium. LPA alone generated 9.9 ± 0.7% transfected SCs po-

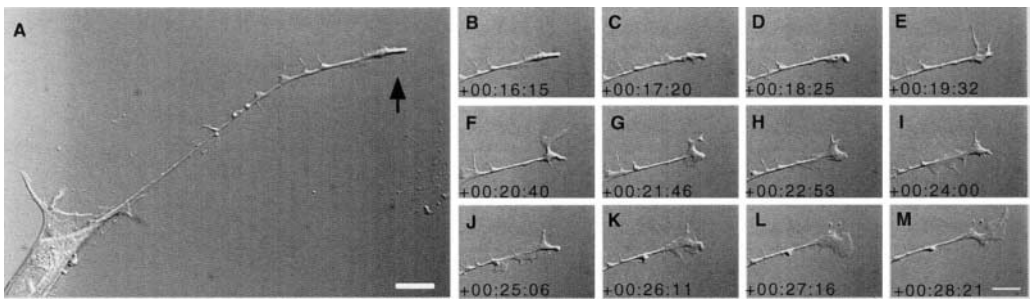

Figure 5. **SC tips display novel growth cone–like behavior.** Isolated SCs were studied using time-lapse live cell imaging. (A, arrow) SC tips displayed dynamic, active remodeling similar to that seen in an axonal growth cone (B–M). Specifically, (E and F) filopodial extensions and (G–M) lamellipodial elaborations were evident. Bars, 10 μm.

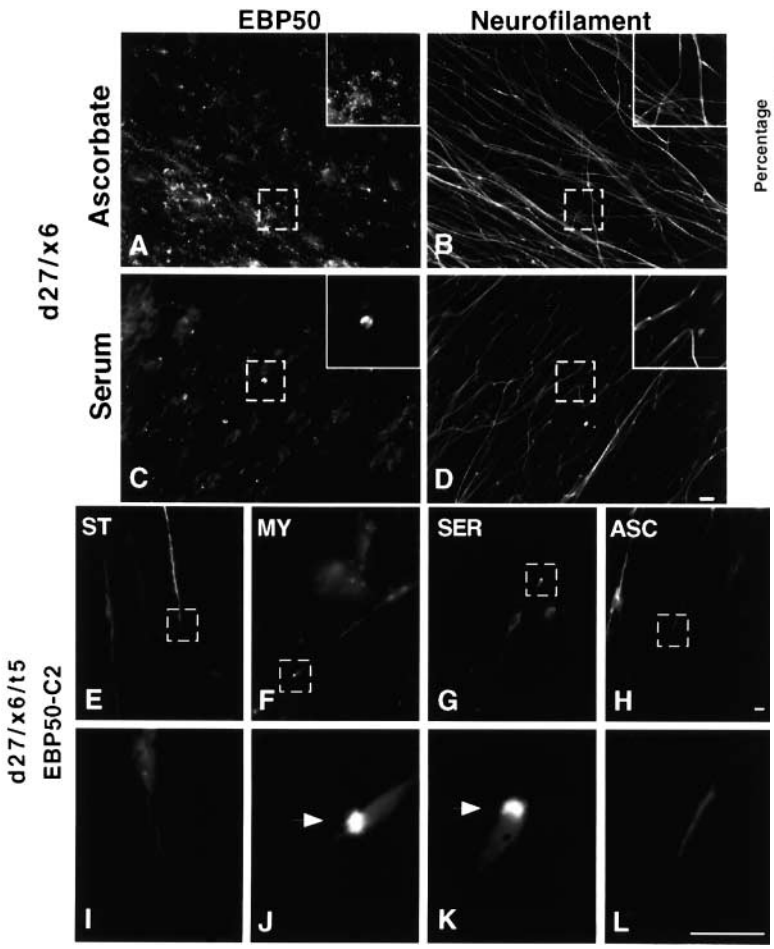

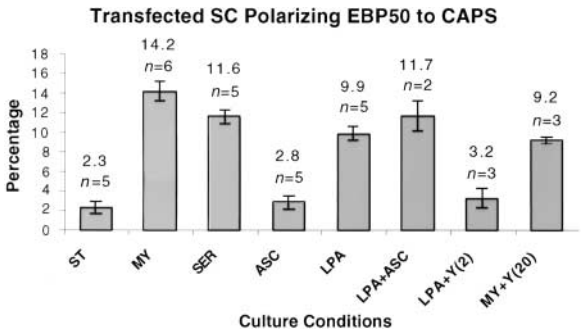

Figure 6. **Cap formation is dependent on serum and can be promoted via Rho stimulation.** At d 21, cultures were supplemented with either serum or ascorbate alone, maintained for 6 d (d27/x6), and stained for (A and C) EBP50 and (B and D) neurofilament. Cap formation was found to be serum dependent. This was also shown with DRG cultures transfected with EBP50-GFP. At d27/x6/t5, various culture conditions were examined as indicated with I–L showing higher magnifications of the outlined regions shown in E–H. EBP50-GFP was found at SC cap structures (arrows) in complete myelin feed (serum + ascorbate; F and J) and cultures supplemented with serum only (G and K). Cultures were also treated with 1 μM LPA to simulate serum stimulation of Rho pathways. Quantitation revealed the presence of serum induced a five- to sixfold increase in the number of caps as compared with standard feed or ascorbate alone. LPA was able to compensate for serum in both the presence and absence of ascorbate. The Rho-kinase inhibitor Y-27632 (Y 2–20 μM, as indicated) was able to block cap formation in the presence of LPA but not complete myelin feed. Data presented as mean ± SEM. *n* equals the number of coverslips analyzed from at least two independent cultures each having two DRGs per coverslip. An average of 423 ± 41 cells per coverslip were counted. Bars, 10 μm.

larizing EBP50-GFP to cap structures, whereas LPA + ascorbate resulted in 11.7 ± 1.6% (Fig. 6).

Downstream effectors implicated in Rho signaling include the Rho-associated kinases (ROCKs), p140mDia, and the phosphatidyl-inositol 4-phosphate 5-kinase (for review see Kaibuchi, 1999). To examine the contribution of the Rho kinases in LPA-induced cap formation, cultures were treated with Y-27632, a pyridine derivative which functions as a specific inhibitor of p160ROCK (ROCKI) and ROCKII (Uehata et al., 1997; Ishizaki et al., 2000). 2 μM of Y-27632 treatment reduced the capacity of LPA to facilitate cap formation to a level similar to that of control cultures maintained in standard feed. Surprisingly, cap formation in cultures maintained in complete myelin feed was reduced by only 35% after 20 μM of Y-27632 treatment (Fig. 6). These results demonstrate that LPA can substitute for serum in cap formation and does so via an Rho-kinase–stimulated pathway. However, the inability of 2–20 μM of Y-27632 to inhibit cap formation in the presence of serum suggests that other pathways may also be operating in this process.

Polarization of microvillar components appears to be an early event in myelination. As microvilli are observed to form contacts with developing nodes of Ranvier, we examined whether SC cap formation was linked to the clustering of proteins at the nodal membrane. Cultures were induced to myelinate under various conditions and myelin segments with associated nodal clusters of ankyrin$_G$ detected by triple staining with antibodies to MBP, ankyrin$_G$, and phospho-ERM (Fig. 7, A–F). 65.6 ± 3.6% of myelin segments exhibited associated ankyrin$_G$ staining at both ends of the segment in cultures treated with both serum and ascorbate. Cultures treated with ascorbate only exhibited 47.2 ± 3.6% of myelin segments with associated ankyrin$_G$ staining and a fourfold increase in the number of myelin segments that showed no associated ankyrin$_G$ staining (17.4 ± 2.8% of myelin segments vs. 4.1 ± 0.8% of segments in cultures treated with serum and ascorbate). In contrast with a previous paper (Eldridge et al., 1987), the average number of myelin segments formed in each culture appeared independent of serum. However, the addition of serum did result in segments of greater average length than those observed in ascorbate alone (Fig. 7, A and D). No clusters of ankyrin$_G$ staining were observed without accompanying phospho-ERM staining (Fig. 7, D–F).

Cultures were also treated with LPA + ascorbate and complete myelin feed containing Y-27632 to determine their effects on node formation. LPA + ascorbate produced moderately similar results as compared with complete myelin feed (8.7% nodal absence, 54.7% nodal presence).

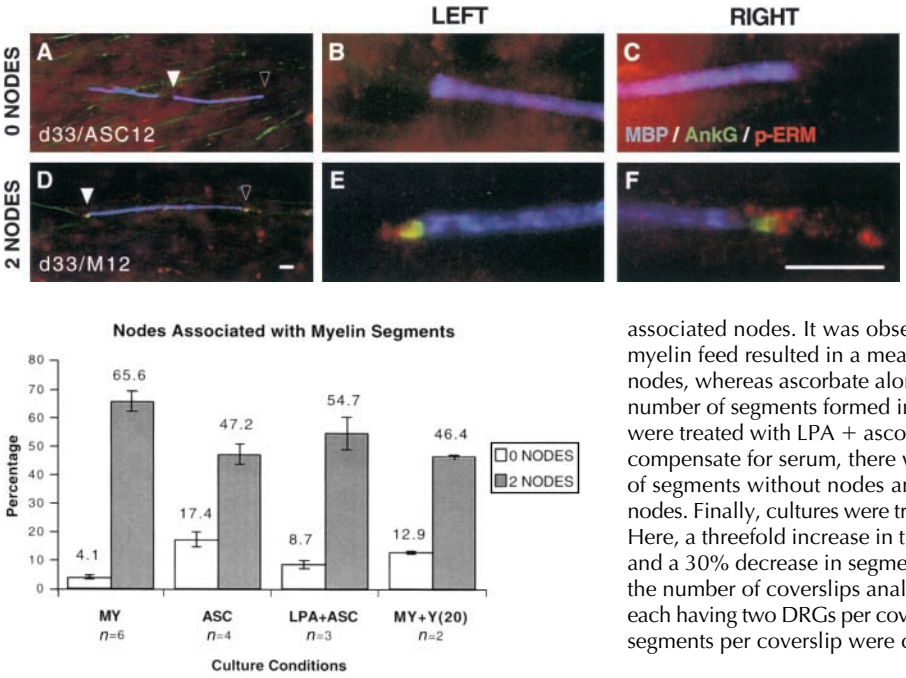

Figure 7. **Efficient node formation is linked to cap formation.** Cultures maintained with either ascorbate alone or complete myelin feed were stained for MBP, AnkG, and phospho-ERM. Myelin segments were identified and each nodal region associated was examined (A and D; closed arrowhead, left-most tip of segment; open arrowhead, right-most tip of segment). Each segment was classified based on the (E and F) presence or (B and C) absence of associated nodes. It was observed that serum stimulation in complete myelin feed resulted in a mean of 1.4 times more segments having two nodes, whereas ascorbate alone produced a fourfold increase in the mean number of segments formed in the absence of nodes. In addition, cultures were treated with LPA + ascorbate. Although LPA was able to moderately compensate for serum, there was a twofold increase in the mean number of segments without nodes and a 16% decrease in segments with two nodes. Finally, cultures were treated with complete myelin feed + Y-27632. Here, a threefold increase in the mean number of segments without nodes and a 30% decrease in segments with two nodes were observed. *n* equals the number of coverslips analyzed from at least two independent cultures each having two DRGs per coverslip. An average of 297 ± 41 (mean ± SEM) segments per coverslip were counted. Bars, 10 μm.

However, there was a twofold increase in the MBP-positive segments formed in the absence of nodes and a 16% decrease in the MBP-positive segments formed in the presence of nodes. This indicates that although LPA can substitute for serum in these cultures, it is not quite as efficient in promoting node formation. The addition of Y-27632 to cultures maintained in myelin feed produced marginal effects on the node–segment association (Fig. 7). Together, these experiments demonstrate that culture conditions promoting formation of SC caps lead to enhanced node formation, supporting the idea of a role for SC microvilli in node formation.

Discussion

Here, we have examined the development of SC microvilli during myelination, in an attempt to understand their potential role in formation of the nodes of Ranvier. We have observed that SCs in DRG explants polarize microvillar components to their distal tips in response to in vitro signals involved in myelin formation, particularly serum addition. We have found that these differentiated SC tips (termed caps) are highly dynamic, growth cone–like structures that result from local activation of ERM proteins downstream of Rho signaling. Finally, we have demonstrated that conditions favoring the formation of SC caps are associated with efficient clustering of membrane proteins at developing nodes of Ranvier.

These observations are summarized in the model shown in Fig. 8. The initial stages of culture establishment include the migration of premyelinating SCs along the radially extended axons emanating from the DRG. These cells appear to be aggressively motile with numerous cell surface microvilli. As the cultures develop, SCs assume their characteristic bipolar myelinating phenotype with microvilli decorating their length. However, treatment of these cultures with serum and

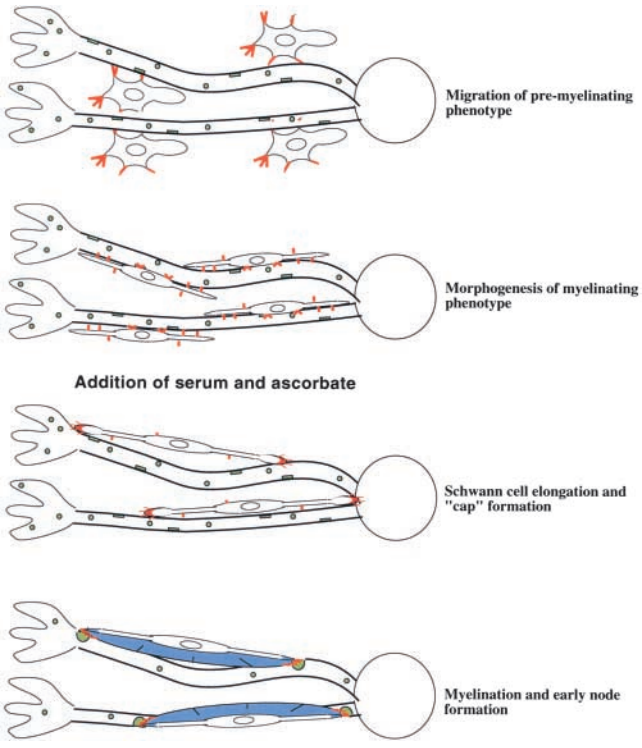

Figure 8. **Model: SC progression toward myelination in DRG explant culture system.** Highly motile, premyelinating SC migrate along axons extending from the DRG. These SC harbor numerous cell surface microvilli (red). Morphogenesis of the SC myelinating phenotype takes place with SCs becoming more longitudinally oriented and axon aligned while retaining many cell surface microvilli. Upon induction, typically using serum and ascorbate, Rho stimulation then leads to the formation of dynamic SC cap structures specifically enriched in activated ERM proteins and other microvillar components (red). Elaboration of the myelin membrane (blue) follows with the clustering of axonal components associated with the formation of early nodes (green).

ascorbate (particularly serum) results in a reorganization of microvillar components into SC caps. Finally, SCs proceed to form myelin sheaths coupled with the clustering of proteins at the nodes of Ranvier.

These results demonstrate a correlative association between the polarization of microvillar components to SC caps and the clustering of ankyrin$_G$, supporting a role for SC microvilli in node formation. Dynamic remodeling of the SC tip associated with cap formation may be important to the efficient clustering of nodal membrane proteins. Hence, nodes might be formed at much slower rates, if at all, in cultures lacking serum where tip dynamics are greatly reduced. Alternatively, the dynamic formation of SC caps and the clustering of ankyrin$_G$ may not be functionally coupled. In this case, serum would be exerting independent effects on these two processes in myelinating cultures. We are currently testing this idea by directly disrupting ERM function and microvilli formation while observing the effects on nodal protein clustering.

SC caps exhibit morphological and dynamic similarities to axonal growth cones. ERM proteins are also observed in axonal growth cones and their activity appears critical to growth cone function (Paglini et al., 1998). SC caps may also have functional similarities to growth cones, potentially playing a role in axon recognition and segregation during early myelination, as well as node formation at later stages. Of importance would be the identification of SC cap proteins that might participate in these processes. These proteins could well be ERM binding proteins such as CD44, which has been implicated in SC-axon adhesion and neuregulin signaling (Sherman et al., 2000). At the node, the cell adhesion molecules neurofascin and NrCAM have been proposed as candidate proteins for the 40–80-nm filaments observed by electron microscopy to link SC microvilli to the nodal membrane (Ichimura and Ellisman, 1991). Perturbing the function of these proteins has been shown to inhibit the clustering of nodal membrane proteins (Lustig et al., 2001). However, potential complementary microvillar receptors for these molecules facilitating SC-axon adhesion remain unknown.

Our data indicate that the addition of serum to DRG explants affects localized changes at SC tips. This might result from concentrations of RhoA that we have observed at the SC tips and/or a potential enrichment of guanine nucleotide exchange factors or guanosine diphosphate dissociation factors at these sites. Given the known effects of Rho on the actin cytoskeleton, it is highly likely that Rho activation at the tip accounts for the dynamic nature of these structures in the presence of serum. As active ERM proteins interact with RhoGDI (guanosine diphosphate dissociation inhibitor; Takahashi et al., 1997), it is likely that ERM activation at the tip will also enhance the formation of active Rho molecules.

As well as local activation of molecules at SC tips, serum may also enhance the movement of vesicle-associated proteins to the tip. For example, exogenous EBP50-GFP is localized to a motile population of punctae in transfected SCs. We have observed that serum causes dramatic changes in SC length and produces significantly longer myelin segments than those formed under serum-free conditions (unpublished data). These findings suggest the potential for functional interdependencies between cap formation, SC elongation and segment length, and effective clustering of nodal membrane proteins.

Materials and methods

DRG explant and SC cultures

DRG explants were cultured essentially as described previously (Howe and McCarthy, 1998). In brief, spinal cords and associated DRGs were dissected out of Wistar rat embryos (embryonic day 16; Charles River) and rinsed in HBSS with 1.2 mM calcium and 0.8 mM magnesium (Sigma-Aldrich) supplemented with 5% FBS, 50 U/ml penicillin, and 50 μg/ml streptomycin. Ganglia were trimmed of spinal roots, removed, and rinsed with HBSS (no serum) and plated into standard feed (basal medium Eagle's [BME]; Sigma-Aldrich) including ITS + supplements (Discovery Labware, Inc.), 0.2% BSA, 10 mM Hepes, 498 mg/dl D-glucose, 100 ng/ml 2.5 S NGF (Discovery Labware, Inc.), 50 U/ml penicillin, and 50 μg/ml streptomycin. Coverslips (Carolina Biologicals) were coated with 0.4 mg/ml Matrigel in BME (Discovery Labware, Inc.) and 10 μg/ml poly-D-lysine (Sigma-Aldrich), and maintained on Teflon circles (American Durafilm). After ~21 d, cultures were supplemented with 15% FBS and 50 μg/ml ascorbate to induce myelination (Eldridge et al., 1987). Cultures were incubated at 37°C in humidified 5% CO_2/95% air with regular feeding every other day. In some instances, media also included various combinations of 1 μM LPA (Sigma-Aldrich) and 2–20 μM Rho-kinase inhibitor, Y-27632 (Calbiochem-Novabiochem).

Isolated SCs were cultured according to the Brockes method (Brockes et al., 1979). P1 rat pups were killed and their sciatic nerves removed. The nerves were incubated with 0.1% collagenase (Sigma-Aldrich) in L-15 for 30 min followed by 0.1% collagenase with 0.25% trypsin for 30 min. After rinsing with DME + 10% FBS, the nerves were triturated and plated into the same media in an untreated 100-mm culture dish. The next day, 10^{-5} M 1-(β-D-arabinofuranosyl) cytosine (AraC; Calbiochem) was added. After 3 d of anti-mitotic treatment, the AraC was washed out and the cells were allowed to recover for 24 h. Anti-Thy1.1 (clone TN-26; 1:100 in DME) and rabbit complement sera HLA-ABC (Sigma-Aldrich; 1:1 in DME) treatment followed to remove residual fibroblasts. Cultures were maintained in Primaria tissue culture flasks (BD Biosciences) with twice weekly feedings of DME + 10% FBS.

EBP50 antibody

An antibody against EBP50 was raised in rabbits for the following study (Covance). A recombinant EBP50-GST fusion was generated (EBP50 cDNA; gift from R. Brian Doctor, University of Colorado Health Sciences Center, Denver, CO) using the pET-41a + vector (Novagen), expressed in bacteria, purified, and used as the immunogen. Antisera were purified using a Talon kit (CLONTECH Laboratories, Inc.), isolated, His-tagged EBP50 (generated using pET-28b + [Novagen]) which was coupled to CNBr Sepharose (Amersham Biosciences). Eluted antibody was dialyzed against PBS followed by 50% glycerol in PBS.

Explant transfection

Explants were transfected using Lipofectamine PLUS (Invitrogen). Cultures were treated for 24 h before transfection with media of choice (Pedraza and Colman, 2000). 1 μg DNA per coverslip was used, and the DNA/PLUS (3.5 μl)/Lipofectamine (2.8 μl) complexes were incubated with the cultures for 3–4 h in unsupplemented BME. The transfection mixture was then removed. The cultures were rinsed once with BME and returned to the appropriate medium.

Immunostaining

Explants were fixed for 10 min at 4°C in 4% PFA/4% sucrose in PBS. After washing with PBS, cultures were blocked with 10% BSA in PBS-T (PBS + 0.2% Triton X-100) for 1 h at 37°C. Primary antibodies were diluted in 2% BSA in PBS-T and incubated for 1–2 h at 37°C. Coverslips were washed with PBS-T; then secondary antibodies, also diluted in 2% BSA in PBS-T (1:1,000), were added and incubated for 1 h at 37°C. After washing with PBS-T, followed by PBS alone and a water rinse, coverslips were mounted using a Vectashield mounting medium (Vector Laboratories). SCs were processed similarly with the exceptions of fixation for 20 min at room temperature followed by a 7-min permeabilization using PBS-T and the omission of Triton X-100 from the proceeding steps. Images were captured using IPLab spectrum software (Signal Analytics Corporation) on an upright Axioplan (Carl Zeiss MicroImaging, Inc.) with a Sensys digital camera (Photometrics Limited), and processed using Adobe Photoshop.

Sources of primary antibodies are as follows: anti-neurofilament (Sternberger Monoclonals, Inc.); anti–α-tubulin (Sigma-Aldrich); anti-ERM and anti–phospho-ezrin (Thr567)/radixin(Thr564)/moesin (Thr558) (Cell Signaling Technology, Inc.); anti-MAG (CHEMICON International, Inc.); anti-MBP (Boehringer); anti-RhoA (Santa Cruz Biotechnology, Inc.); Alexa-Fluor 594 phalloidin (Molecular Probes); anti-βIV spectrin (a gift from M. Komada, Tokyo Institute of Technology, Tokyo, Japan; Komada and Soriano, 2002); anti-ERM (a gift from E. Luna, University of Massachusetts Medical School, Worcester, MA); anti-ankyrin$_G$ (Lambert et al., 1997); and anti-EBP50 as described above (EBP50 antibody). All secondary antibodies were purchased from Molecular Probes.

Live cell imaging

Explants or dispersed SCs were grown on either 22-mm square coverslips or 30-mm Rose dishes (World Precision Instruments) and treated as indicated. Preparations were mounted for imaging on an inverted microscope (DMIRE 2; Leica) in a 37°C-heated 5% CO_2/95% room air plexiglass environmental chamber. Image acquisition and processing was performed using an extended range cooled CCD camera (ORCA ER; Hamamatsu) and OpenLab software (Improvision).

Online supplemental material

The original time-lapse videos from which the still images presented in Fig. 3 were taken are available for viewing as supplemental material. Video 1 contains time-lapse fluorescence microscopy of an EBP50-GFP–transfected SC maintained in standard feed. Video 2 specifically shows the distal tip of this cell. Video 3 shows time-lapse fluorescence microscopy of an EBP50-GFP–transfected SC after the induction of myelination using serum and ascorbate. Video 4 shows the remodeling EBP50 enriched tip of this cell. Videos are available at http://www.jcb.org/cgi/content/full/jcb.200303039/DC1.

We would like to thank Joshua Nordberg for superior technical assistance and Greenfield Sluder for advice and helpful discussion regarding live cell imaging.

These studies were supported by the National Institutes of Health grant RO1NS36637 (to S. Lambert) and by the Neuroscience Training grant 5T32NS07366 (to C. Gatto). We would also like to acknowledge the National Center for Research Resources Shared Equipment grant (1S10RR15775) used to purchase the microscopy system used in the live cell imaging studies presented.

Submitted: 6 March 2003
Accepted: 11 June 2003

References

Arroyo, E.J., and S.S. Scherer. 2000. On the molecular architecture of myelinated fibers. *Histochem. Cell Biol.* 113:1–18.

Berghs, S., D. Aggujaro, R. Dirkx, Jr., E. Maksimova, P. Stabach, J.M. Hermel, J.P. Zhang, W. Philbrick, V. Slepnev, T. Ort, and M. Solimena. 2000. βIV spectrin, a new spectrin localized at axon initial segments and nodes of ranvier in the central and peripheral nervous system. *J. Cell Biol.* 151:985–1002.

Brockes, J.P., K.L. Fields, and M.C. Raff. 1979. Studies on cultured rat Schwann cells. I. Establishment of purified populations from cultures of peripheral nerve. *Brain Res.* 165:105–118.

Ching, W., G. Zanazzi, S.R. Levinson, and J.L. Salzer. 1999. Clustering of neuronal sodium channels requires contact with myelinating Schwann cells. *J. Neurocytol.* 28:295–301.

Davis, J.Q., S. Lambert, and V. Bennett. 1996. Molecular composition of the node of Ranvier: identification of ankyrin-binding cell adhesion molecules neurofascin (mucin+/third FNIII domain−) and NrCAM at nodal axon segments. *J. Cell Biol.* 135:1355–1367.

Deerinck, T.J., S.R. Levinson, G.V. Bennett, and M.H. Ellisman. 1997. Clustering of voltage-sensitive sodium channels on axons is independent of direct Schwann cell contact in the dystrophic mouse. *J. Neurosci.* 17:5080–5088.

Eldridge, C.F., M.B. Bunge, R.P. Bunge, and P.M. Wood. 1987. Differentiation of axon-related Schwann cells in vitro. I. Ascorbic acid regulates basal lamina assembly and myelin formation. *J. Cell Biol.* 105:1023–1034.

Gary, R., and A. Bretscher. 1995. Ezrin self-association involves binding of an N-terminal domain to a normally masked C-terminal domain that includes the F-actin binding site. *Mol. Biol. Cell.* 6:1061–1075.

Howe, D.G., and K.D. McCarthy. 1998. A dicistronic retroviral vector and culture model for analysis of neuron-Schwann cell interactions. *J. Neurosci. Methods.* 83:133–142.

Ichimura, T., and M.H. Ellisman. 1991. Three-dimensional fine structure of cytoskeletal-membrane interactions at nodes of Ranvier. *J. Neurocytol.* 20:667–681.

Ishizaki, T., M. Uehata, I. Tamechika, J. Keel, K. Nonomura, M. Maekawa, and S. Narumiya. 2000. Pharmacological properties of Y-27632, a specific inhibitor of rho-associated kinases. *Mol. Pharmacol.* 57:976–983.

Jessen, K.R., A. Brennan, L. Morgan, R. Mirsky, A. Kent, Y. Hashimoto, and J. Gavrilovic. 1994. The Schwann cell precursor and its fate: a study of cell death and differentiation during gliogenesis in rat embryonic nerves. *Neuron.* 12:509–527.

Kaibuchi, K. 1999. Regulation of cytoskeleton and cell adhesion by Rho targets. *Prog. Mol. Subcell. Biol.* 22:23–38.

Kaplan, M.R., A. Meyer-Franke, S. Lambert, V. Bennett, I.D. Duncan, S.R. Levinson, and B.A. Barres. 1997. Induction of sodium channel clustering by oligodendrocytes. *Nature.* 386:724–728.

Komada, M., and P. Soriano. 2002. [β]IV-spectrin regulates sodium channel clustering through ankyrin-G at axon initial segments and nodes of Ranvier. *J. Cell Biol.* 156:337–348.

Kordeli, E., J. Davis, B. Trapp, and V. Bennett. 1990. An isoform of ankyrin is localized at nodes of Ranvier in myelinated axons of central and peripheral nerves. *J. Cell Biol.* 110:1341–1352.

Kordeli, E., S. Lambert, and V. Bennett. 1995. AnkyrinG. A new ankyrin gene with neural-specific isoforms localized at the axonal initial segment and node of Ranvier. *J. Biol. Chem.* 270:2352–2359.

Lambert, S., J.Q. Davis, and V. Bennett. 1997. Morphogenesis of the node of Ranvier: co-clusters of ankyrin and ankyrin-binding integral proteins define early developmental intermediates. *J. Neurosci.* 17:7025–7036.

Lustig, M., G. Zanazzi, T. Sakurai, C. Blanco, S.R. Levinson, S. Lambert, M. Grumet, and J.L. Salzer. 2001. Nr-CAM and neurofascin interactions regulate ankyrin G and sodium channel clustering at the node of Ranvier. *Curr. Biol.* 11:1864–1869.

Martini, R., and M. Schachner. 1986. Immunoelectron microscopic localization of neural cell adhesion molecules (L1, N-CAM, and MAG) and their shared carbohydrate epitope and myelin basic protein in developing sciatic nerve. *J. Cell Biol.* 103:2439–2448.

Martini, R., and M. Schachner. 1988. Immunoelectron microscopic localization of neural cell adhesion molecules (L1, N-CAM, and myelin-associated glycoprotein) in regenerating adult mouse sciatic nerve. *J. Cell Biol.* 106:1735–1746.

Matsui, T., M. Maeda, Y. Doi, S. Yonemura, M. Amano, K. Kaibuchi, and S. Tsukita. 1998. Rho-kinase phosphorylates COOH-terminal threonines of ezrin/radixin/moesin (ERM) proteins and regulates their head-to-tail association. *J. Cell Biol.* 140:647–657.

Melendez-Vasquez, C.V., J.C. Rios, G. Zanazzi, S. Lambert, A. Bretscher, and J.L. Salzer. 2001. Nodes of Ranvier form in association with ezrin-radixin-moesin (ERM)-positive Schwann cell processes. *Proc. Natl. Acad. Sci. USA.* 98:1235–1240.

Paglini, G., P. Kunda, S. Quiroga, K. Kosik, and A. Caceres. 1998. Suppression of radixin and moesin alters growth cone morphology, motility, and process formation in primary cultured neurons. *J. Cell Biol.* 143:443–455.

Pedraza, L., and D.R. Colman. 2000. Fluorescent myelin proteins provide new tools to study the myelination process. *J. Neurosci. Res.* 60:697–703.

Reczek, D., and A. Bretscher. 1998. The carboxyl-terminal region of EBP50 binds to a site in the amino-terminal domain of ezrin that is masked in the dormant molecule. *J. Biol. Chem.* 273:18452–18458.

Reczek, D., M. Berryman, and A. Bretscher. 1997. Identification of EBP50: a PDZ-containing phosphoprotein that associates with members of the ezrin-radixin-moesin family. *J. Cell Biol.* 139:169–179.

Ritchie, J.M., and R.B. Rogart. 1977. Density of sodium channels in mammalian myelinated nerve fibers and nature of the axonal membrane under the myelin sheath. *Proc. Natl. Acad. Sci. USA.* 74:211–215.

Scherer, S.S., and E.J. Arroyo. 2002. Recent progress on the molecular organization of myelinated axons. *J. Peripher. Nerv. Syst.* 7:1–12.

Scherer, S.S., T. Xu, P. Crino, E.J. Arroyo, and D.H. Gutmann. 2001. Ezrin, radixin, and moesin are components of Schwann cell microvilli. *J. Neurosci. Res.* 65:150–164.

Shaw, R.J., M. Henry, F. Solomon, and T. Jacks. 1998. RhoA-dependent phosphorylation and relocalization of ERM proteins into apical membrane/actin protrusions in fibroblasts. *Mol. Biol. Cell.* 9:403–419.

Sherman, L.S., T.A. Rizvi, S. Karyala, and N. Ratner. 2000. CD44 enhances neu-

regulin signaling by Schwann cells. *J. Cell Biol.* 150:1071–1084.

Shrager, P. 1989. Sodium channels in single demyelinated mammalian axons. *Brain Res.* 483:149–154.

Takahashi, K., T. Sasaki, A. Mammoto, K. Takaishi, T. Kameyama, S. Tsukita, and Y. Takai. 1997. Direct interaction of the Rho GDP dissociation inhibitor with ezrin/radixin/moesin initiates the activation of the Rho small G protein. *J. Biol. Chem.* 272:23371–23375.

Trapp, B.D., S.B. Andrews, A. Wong, M. O'Connell, and J.W. Griffin. 1989. Co-localization of the myelin-associated glycoprotein and the microfilament components, F-actin and spectrin, in Schwann cells of myelinated nerve fibres. *J. Neurocytol.* 18:47–60.

Uehata, M., T. Ishizaki, H. Satoh, T. Ono, T. Kawahara, T. Morishita, H. Tamakawa, K. Yamagami, J. Inui, M. Maekawa, and S. Narumiya. 1997. Calcium sensitization of smooth muscle mediated by a Rho-associated protein kinase in hypertension. *Nature.* 389:990–994.

Vabnick, I., S.D. Novakovic, S.R. Levinson, M. Schachner, and P. Shrager. 1996. The clustering of axonal sodium channels during development of the peripheral nervous system. *J. Neurosci.* 16:4914–4922.

Weiner, J.A., N. Fukushima, J.J. Contos, S.S. Scherer, and J. Chun. 2001. Regulation of Schwann cell morphology and adhesion by receptor-mediated lysophosphatidic acid signaling. *J. Neurosci.* 21:7069–7078.

Yonemura, S., T. Matsui, and S. Tsukita. 2002. Rho-dependent and -independent activation mechanisms of ezrin/radixin/moesin proteins: an essential role for polyphosphoinositides in vivo. *J. Cell Sci.* 115:2569–2580.